JOURNAL OF COMPUTATIONAL PHYSICS 7, 367–384 (1971)

Pair Distribution in the Classical Rigid Disk and Sphere Systems

FRANK H. STILLINGER

Bell Telephone Laboratories, Incorporated, Murray Hill, New Jersey 07974

Received November 10, 1970

Relatively simple geometric criteria are used to locate singularities (with respect to variable r_{12}) of the rigid disk and sphere pair distribution function $\rho^{(2)}(\mathbf{r}_1, \mathbf{r}_2)$. Some singularities which arise in low density order are classified and tabulated. It is argued that the existence of random disk and sphere packings causes the singularities to occur densely for all r_{12}. Thus $\rho^{(2)}$ is nowhere analytic in this variable. Implications of this result are pointed out for both computational and analytical statistical mechanics of the disk and sphere models.

1. INTRODUCTION

In order for the practitioners of statistical mechanics to appreciate and exhibit the power of that discipline, they have found it necessary to exploit special models. Among the most popular of these models for molecules in interaction have been the rigid sphere system and its two-dimensional rigid disk analog. The reasons for their popularity lie partly in analytic tractability (relatively speaking!), partly in the helpful ease with which accessible molecular arrangements can be visualized, but largely in the ability of these models to demonstrate both fluid and solid phase properties along with a freezing transition [1, 2].

Research on the equilibrium properties of rigid disk and sphere systems fortunately has achieved wide-ranging success. In the low density regime, accurate virial coefficients are now available (through the seventh [3]). At the other extreme, high compression expansions have been developed both analytically [4, 5] and computationally [6, 7]. Our general grasp of the behavior of these models furthermore has been enriched by the "scaled particle" theory, [8, 9] and by the related closed-form solution to the hard-sphere Percus–Yevick integral equation [10].

The rigid sphere and disk equilibrium pair distribution functions form the object of scrutiny in this paper. In particular, we shall examine the distribution of these functions' singularities in their spatial variable r_{12}. Implications of the results for the future course of both analytical and computational work on these systems will be stressed at the appropriate points in Section 6.

2. Formal Relations

The grand ensemble provides the most convenient context in which to carry out our analysis. We start with the general expression for the pair distribution function $\rho^{(2)}(\mathbf{r}_1, \mathbf{r}_2)$ for particles whose interaction potential is $\Phi_N(\mathbf{r}_1 \cdots \mathbf{r}_N)$:

$$\rho^{(2)}(\mathbf{r}_1, \mathbf{r}_2) = \exp(\beta\Omega) \sum_{N=2}^{\infty} \frac{y^N}{(N-2)!} \int d\mathbf{r}_3 \cdots \int d\mathbf{r}_N \exp[-\beta\Phi_N(1 \cdots N)],$$
$$\beta = (k_B T)^{-1}. \tag{2.1}$$

The absolute activity is denoted here by y:

$$y = \exp(\beta\mu)/\lambda^d, \tag{2.2}$$

where μ is the chemical potential, λ is the mean thermal de Broglie wavelength, and d is the system dimensionality. The position integrals in Eq. (2.1) span the system region, which we will denote by V both for disks ($d = 2$) and spheres ($d = 3$). The grand partition function itself is given by the expression:

$$\exp(-\beta\Omega) = 1 + \sum_{N=1}^{\infty} \frac{y^N}{N!} \int d\mathbf{r}_1 \cdots \int d\mathbf{r}_N \exp[-\beta\Phi_N(\mathbf{r}_1 \cdots \mathbf{r}_N)]$$
$$= 1 + \sum_{N=1}^{\infty} \frac{y^N}{N!} Z_N . \tag{2.3}$$

The rigid sphere and disk models are special cases of the class of systems with pairwise-additive interactions:

$$\Phi_N(1 \cdots N) = \sum_{i<j=1}^{N} \varphi(r_{ij}). \tag{2.4}$$

For both spheres and disks we shall denote the collision diameter by a, so for these models

$$\begin{aligned} &\varphi(r) \to +\infty, \qquad && r < a, \\ &\varphi(r) = 0, && r \geqslant a. \end{aligned} \tag{2.5}$$

The $\rho^{(2)}$ expression (2.1) may then be rearranged somewhat:

$$\rho^{(2)}(\mathbf{r}_1, \mathbf{r}_2) = y^2 \exp[-\beta\varphi(r_{12})]$$
$$\times \left\{\left(1 + \sum_{N=1}^{\infty} \frac{y^N}{N!} X_N(\mathbf{r}_1, \mathbf{r}_2)\right) \Big/ \left(1 + \sum_{N=1}^{\infty} \frac{y^N}{N!} Z_N\right)\right\}, \tag{2.6}$$

where we have introduced the set of configuration integrals

$$X_N(\mathbf{r}_1, \mathbf{r}_2) = \int d\mathbf{r}_3 \cdots \int d\mathbf{r}_{N+2} \exp\left\{-\beta \sum_{j=3}^{N+2} [\varphi(1j) + \varphi(2j)] - \beta \sum_{i<j=3}^{N+2} \varphi(ij)\right\} \quad (2.7)$$

for N particles in V moving under the influence of two other fixed particles.

Our present interest lies in the case that V is very large compared to the particle size in all d directions. Thus, we may suppose that both $\mathbf{r}_1$ and $\mathbf{r}_2$ are far from the boundary of V, so that at low density, $\rho^{(2)}$ will depend spatially only on $r_{12} = |\mathbf{r}_2 - \mathbf{r}_1|$.

It is known that the activity power series for the grand potential Ω and the distribution function $\rho^{(2)}$ for rigid disks and spheres have nonzero convergence radii in the $V \to \infty$ limit [11]. We can therefore be assured that a y power series development of the last factor in Eq. (2.6) will have coefficients that approach physically meaningful limits as $V \to \infty$. Specifically, one finds

$$\begin{aligned} y^{-2} \exp[\beta\varphi(r_{12})]\, \rho^{(2)}(\mathbf{r}_1, \mathbf{r}_2) \\ & 1 + y\{X_1(\mathbf{r}_1, \mathbf{r}_2) - Z_1\} \\ & + \frac{y^2}{2!}\{X_2(\mathbf{r}_1, \mathbf{r}_2) - 2Z_1X_1(\mathbf{r}_1, \mathbf{r}_2) - [Z_2 - 2(Z_1)^2]\} \\ & + \frac{y^3}{3!}\{X_3(\mathbf{r}_1, \mathbf{r}_2) - 3Z_1X_2(\mathbf{r}_1, \mathbf{r}_2) - 3[Z_2 - 2(Z_1)^2]\, X_1(\mathbf{r}_1, \mathbf{r}_2) \\ & \qquad - [Z_3 - 6Z_2Z_1 + 6(Z_1)^3]\} \\ & + \frac{y^4}{4!}\{X_4(\mathbf{r}_1, \mathbf{r}_2) - 4Z_1X_3(\mathbf{r}_1, \mathbf{r}_2) - 6[Z_2 - 2(Z_1)^2]\, X_2(\mathbf{r}_1, \mathbf{r}_2) \\ & \qquad - 4[Z_3 - 6Z_2Z_1 + 6(Z_1)^3]\, X_1(\mathbf{r}_1, \mathbf{r}_2) \\ & \qquad - [Z_4 - 8Z_3Z_1 - 6(Z_2)^2 + 36Z_2(Z_1)^2 - 24(Z_1)^4]\} \\ & + \cdots \end{aligned} \quad (2.8)$$

Although it is straightforward to write down the general coefficient in Eq. (2.8), that would be pointless for present purposes. We need merely to note that the y^n coefficient consists of a linear combination of the X_j's, where $j \leqslant n$, and where the coefficient of X_n is precisely $(n!)^{-1}$. The particular combinations of X_j and Z_k products which occur following X_n are present to assure proper $V \to \infty$ limit behavior, since in dominant order

$$X_n(\mathbf{r}_1, \mathbf{r}_2) \propto V^n \qquad \text{as} \quad V \to \infty. \quad (2.9)$$

3. One-Particle Integrals

In order to illustrate the foregoing general formalism, we now examine X_1 for disks and spheres. The results in themselves merely repeat what has long been known for the low-density (i.e., small y) $\rho^{(2)}$ behavior, especially via Mayer cluster theory [12]. However it is valuable to cover this ground again to provide a proper orientation for examination of higher-order terms in the next section.

The shape of V is largely irrelevant, though for the sake of concreteness it may be visualized as a rectangle ($d = 2$) or rectangular solid ($d = 3$). We have

$$X_1(\mathbf{r}_1, \mathbf{r}_2) = \int_V d\mathbf{r}_3 \exp[-\beta\varphi(r_{13}) - \beta\varphi(r_{23})], \tag{3.1}$$

which for disks and spheres gives precisely the volume (or area) within V over which the center of particle 3 is free to move. As Fig. 1 shows, two cases must be distinguished for both $d = 2$ and 3; namely $0 \leqslant r_{12} \leqslant 2a$, and $2a < r_{12}$. The difference is simply that the exclusion region generated by infinite repulsions

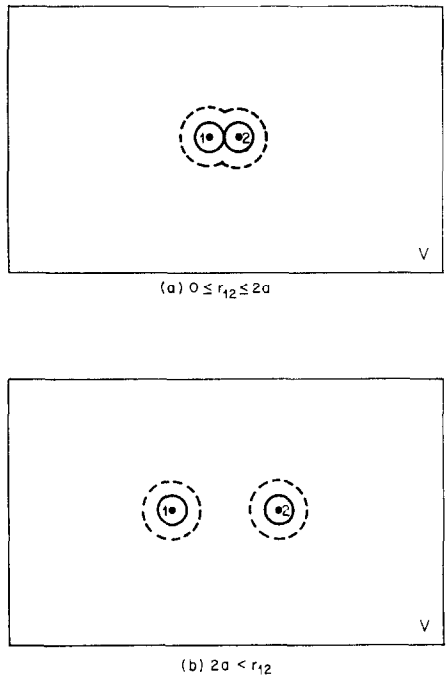

Fig. 1. Region available to particle 3 in integral $X_1(\mathbf{r}_1, \mathbf{r}_2)$, Eq. (3.1). The rigid-particle repulsions with fixed particles 1 and 2 exclude a singly-connected region (dotted outline) in case (a), but for case (b) this exclusion region is unconnected.

between 1 and 3, and 2 and 3, is connected in the former case, but disconnected in the latter case.

One readily calculates for rigid disks that

$$X_1(\mathbf{r}_1, \mathbf{r}_2) = V - \pi a^2 - r_{12}\sqrt{a^2 - \tfrac{1}{4}r_{12}^2} - 2a^2 \sin^{-1}(r_{12}/2a), \qquad 0 \leqslant r_{12} \leqslant 2a,$$

$$= V - 2\pi a^2, \qquad 2a < r_{12}. \tag{3.2}$$

The analogous rigid sphere result is

$$X_1(\mathbf{r}_1, \mathbf{r}_2) = V - \frac{4\pi}{3}a^3 - \pi a^2 r_{12} + \frac{\pi}{12}r_{12}^3, \qquad 0 \leqslant r_{12} \leqslant 2a,$$

$$= V - \frac{8\pi}{3}a^3, \qquad 2a < r_{12}. \tag{3.3}$$

Of course, also have

$$Z_1 = V \tag{3.4}$$

for both disks and spheres, so that the full coefficient $X_1 - Z_1$ of y in expression (2.8) is independent of V.

Within each of the two ranges $0 \leqslant r_{12} < 2a$, and $2a < r_{12}$, both the disk and sphere integrals X_1 are analytic functions of the spatial variable r_{12}. The point $r_{12} = 2a$ though is clearly a singular point at which the second derivatives of both fail to exist. It is obvious that this singular point is directly associated with the change in connectivity of the boundary within which the movable particle 3 must remain. The singular configuration separating the two cases is one which just permits the movable particle to fit between the other two fixed particles.

4. Singularities of Higher Integrals

The integrals X_n rapidly increase in complexity as n, the number of movable particles involved, increases beyond one. No general technique is available for their exact evaluation, unfortunately. But such evaluations are not required if one's goal is the more modest identification of the singular points in the r_{12} variation of the y^n coefficient in expansion (2.8). These singularities may be located by relatively simple geometric means. At least when one is within the convergence radius (in the y plane) of that expansion, the set of all these singularities for $r_{12} \geqslant a$ will be precisely the singularities of $\rho^{(2)}(r_{12})$.

Equation (2.7) shows for disks and spheres that X_n equals the content of the entire (dn)-dimensional accessible configuration space region $\mathbf{R}_n$ for the n movable

particles. $\mathbf{R}_n$ is bounded by a set of $(dn - 1)$-dimensional hypersurfaces that correspond to the following special configuration conditions:

(a) contact of any one of the n movable particles with the wall of V;

(b) contact between any one of the movable particles, and either of fixed particles 1 and 2;

(c) contact between any pair of movable particles.

In the case $n = 1$ treated explicitly in the preceding section, only (a) and (b) are relevant of course; the singularity noted there at $r_{12} = 2a$ concerned the change from intersection (when $0 \leqslant r_{12} \leqslant 2a$) to nonintersection ($2a < r_{12}$) of the surfaces (b). For general n, we must expect the geometric relationships between the hypersurfaces of classes (b) and (c) to change as r_{12} varies. The result will be that several r_{12} intervals, or "cases", will be generated within each of which analytic behavior in r_{12} will obtain, and the endpoints of which will be singular points of Z_n, and therefore also $\rho^{(2)}$.

We now separately examine the situations for several small n values.

$n = 2$

The singularity in $X_1(\mathbf{r}_1, \mathbf{r}_2)$ at $r_{12} = 2a$ corresponds to exact fitting of a movable particle 3 between fixed particles 1 and 2. For larger r_{12} simultaneous contacts (13) and (23) are impossible. The same situation applies separately to the two movable particles 3 and 4 involved in $X_2(\mathbf{r}_1, \mathbf{r}_2)$. The separation $r_{12} = 2a$ is the maximum which permits simultaneous contacts (13) and (23) [or alternatively (14) and (24)]. As r_{12} increases across this value the corresponding pairs of hypersurfaces in class (b) above become disconnected on the boundary of $\mathbf{R}_2$. Therefore, the one-particle singularity $r_{12} = 2a$ is repeated for the two-particle $X_2(\mathbf{r}_1, \mathbf{r}_2)$.

Repetition of singularities encountered in lower orders will be a universal trait for arbitrary n. It simply reflects the geometric behavior of proper subsets of the n movable particles in their tendency to reiterate previously encountered behavior. Of course new singular r_{12} values are also to be expected in each succeeding n order.

Movable particles 3 and 4 can form a chain of simultaneous contacts such as (13)(34)(42) between 1 and 2, but only if $r_{12} \leqslant 3a$. If $r_{12} > 3a$ however, these simultaneous contacts are obviously impossible. The boundary of $(2d)$-dimensional region $\mathbf{R}_2$ has therefore changed in a fundamental way as r_{12} crosses $3a$, since below this value contact hypersurfaces (13), (34), and (42) have common points, but above this value they do not. Consequently $r_{12} = 3a$ must be a singular point of X_2. Figure 2(a) shows the singular configuration.

Another singular r_{12} value arises for $n = 2$, which is illustrated in Fig. 2(b). The reason for this singularity, at $r_{12} = 3^{1/2}a$, is very clearly that two parallel

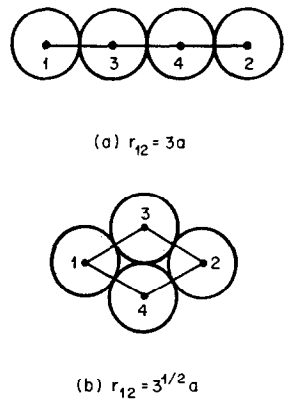

FIG. 2. Singular configurations for X_3. In (a), we have a two-particle chain which can just stretch between fixed particles 1 and 2 when $r_{12} = 3a$; a second possibility with 3 and 4 interchanged also exists. Configuration (b) requires simultaneous contacts between (13), (32), (14), and (42), and produces a singularity at $r_{12} = 3^{1/2}a$; for larger r_{12} two parallel contact chains are impossible.

contact chains (13)(32) and (14)(42) are impossible for larger r_{12}. Thus the boundary of $\mathbf{R}_2$ only has points common to all the hypersurfaces (13), (32), (14), and (42) when $r_{12} \leqslant 3^{1/2}a$. For larger r_{12}, the bounding surface set topology of $\mathbf{R}_2$ is fundamentally different.

Nijboer and Van Hove [13] have evaluated the rigid sphere $\rho^{(2)}$ via cluster theory through terms proportional to the square of the density. This is directly equivalent to order y^2 in our expression (2.8), for which X_1 and X_2 are required. Their results in fact show precisely the values:

$$r_{12} = 2a, \qquad 3^{1/2}a, \qquad 3a \tag{4.1}$$

to be those at which singularities occur, in agreement with the present analysis.

$n = 3$

Consistent with previous remarks, we expect $2a$, $3^{1/2}$, and $3a$ also to be singular r_{12} values for $X_3(\mathbf{r}_1, \mathbf{r}_2)$. But since these values arise from interactions of less than the full set of movable particles, we can confine attention to situations simultaneously involving all three movable particles 3, 4, and 5.

The simplest possibility is surely the single contact chain spanning the space between fixed particles 1 and 2 [see Fig. 3(a)]. Each of the $3! = 6$ possible single contact chains can exist only when $r_{12} \leqslant 4a$, so the upper limit $r_{12} = 4a$ will be a singular point. The obvious generalization is that the point $r_{12} = (n + 1)a$ will be singular in X_n, since it is the maximum extension possible for the single contact chain.

Figure 3(b) shows a second possibility, involving a sort of hybrid chain. This case

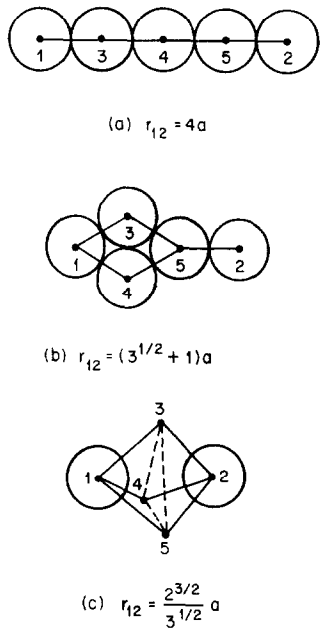

FIG. 3. Singular configurations for X_3. Both (a) and (b) are relevant to disks and spheres, while (c) refers to spheres alone. For clarity, only the centers of the three movable spheres are shown in (c).

has two parallel paths of contacts in series with a single path. The six possible sets of contacts giving rise to this structure are

$$\begin{aligned}
&(13)(14)(35)(45)(52),\\
&(13)(15)(34)(54)(42),\\
&(14)(15)(43)(53)(32),\\
&(13)(34)(35)(42)(52),\\
&(14)(43)(45)(32)(52),\\
&(15)(53)(54)(32)(42).
\end{aligned} \tag{4.2}$$

For each of these, $r_{12} = (3^{1/2} + 1)a$ is the maximum possible extension. When r_{12} exceeds this singular upper limit, the boundary of $\mathbf{R}_3$ will suddenly contain no points common to the quintets of hypersurfaces shown in (4.2).

With $n = 3$ we encounter for the first time a distinction between disks and spheres, so far as singular r_{12} values are concerned. Only the latter can accommodate three parallel contact chains between fixed particles 1 and 2. Figure 3(c) provides

the relevant illustration, and one easily verifies that the corresponding singularity occurs at

$$r_{12} = (2^{3/2}/3^{1/2})a. \tag{4.3}$$

$n = 4$

Several singular r_{12} values that arise for the first time when $n = 4$ represent straightforward extensions of earlier cases. They are exhibited in Fig. 4. The

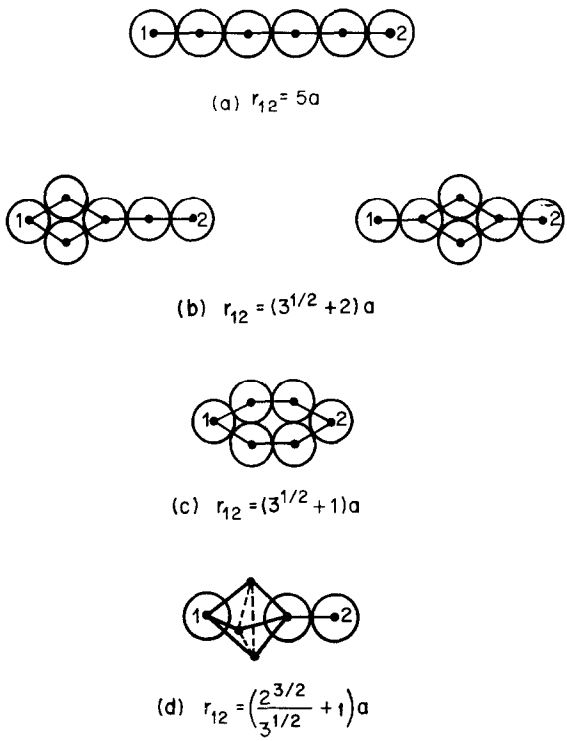

FIG. 4. Some singular X_4 configurations. These are all obtained by interposing one or more particles in earlier cases. Structure (d) refers to spheres only.

single chain (Fig. 4(a)) of course produces singular X_4 behavior at $r_{12} = 5a$. The chain with one doubled section (Fig. 4(b)) generates a singularity at $r_{12} = (3^{1/2} + 2)a$. The case of two parallel chains, each involving two movable particles is shown in Fig. 4(c); it merely reinforces the earlier singularity of Fig. 3(b), albeit with a somewhat different structure. Figure 4(d) refers only to rigid spheres, and trivially extends structure Fig. 3(c) by interposing another particle between 1 and 2.

Although we do not display it in a figure, it is clear that rigid spheres will also have a singularity associated with four parallel chains. The resulting octahedral arrangement corresponds to

$$r_{12} = 2^{1/2}a. \tag{4.4}$$

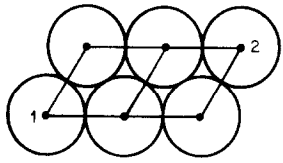

(a) $3^{1/2}a \leq r_{12} \leq 7^{1/2}a$

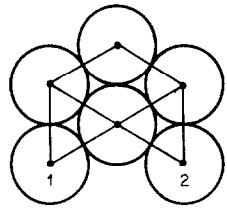

(b) $3^{1/2}a \leq r_{12} \leq 2a$

FIG. 5. Further contact sets for four movable disks or spheres.

Figure 5(a) illustrates a choice of simultaneous contacts with $n = 4$ that generates yet another singular r_{12} value (for both disks and spheres). It is possible to maintain these contacts, denoted in the figure by solid lines, only when

$$3^{1/2}a \leqslant r_{12} \leqslant 7^{1/2}a. \tag{4.5}$$

Of course the lower limit has already been encountered for $n = 2$ [see Fig. 2(b)]. The singular distances

$$r_{12} = 3^{1/2}a,\ 2a,\ 7^{1/2}a \tag{4.6}$$

in fact represent second, third, and fourth neighbor separations in the close-packed hexagonal disk lattice. In succeeding n orders we can expect singularities to be identified with fifth, sixth, seventh, $\cdots$ neighbor distances in the same lattice.

As we have seen before, certain contact set choices tend only to repeat earlier

singular r_{12} values, without giving any new information. Figure 5(b) shows such a case for $n = 4$, where the required contacts (the solid lines) are possible only if

$$3^{1/2}a \leqslant r_{12} \leqslant 2a. \tag{4.7}$$

An exhaustive survey indeed demonstrates that no further singularities for $n = 4$ remain to be uncovered for rigid disks.

Two more singularities are possible for rigid spheres alone, however. They pertain to the nonplanar contact configurations presented in Fig. 6. In its most extended form, the first of these in Fig. 6(a) forces the four movable spheres into a

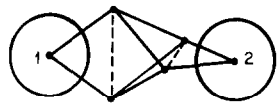

(a) $2^{1/2}a \leq r_{12} \leq (3^{1/2} + 2^{-1/2})a$

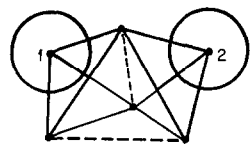

(b) $r_{12} \leq (5/3)a$

FIG. 6. Rigid sphere singularities for $n = 4$. Only the centers have been shown for the movable spheres. Solid lines indicate the required contacts. For both (a) and (b) the maximum extension, which generates the respective singularities, forces movable particles into a regular tetrahedral configuration. The dotted lines locate tetrahedron edges not included in the starting contact set.

regular tetrahedral arrangement, and the implied singularitiy occurs at

$$r_{12} = (3^{1/2} + 2^{-1/2})a. \tag{4.8}$$

The other case, in Fig. 6(b), likewise forces the movable particles into a regular tetrahedral configuration when r_{12} is maximized; now, however, particles 1 and 2 are located above two tetrahedral faces, and the singularity lies at

$$r_{12} = (5/3)a. \tag{4.9}$$

$n = 5$

Table I collects the singular r_{12}/a values thus far inferred for $n \leqslant 4$. It is clear from that table that the number of singularities to be encountered in succeeding orders increases very rapidly. For that reason we shall not attempt to compile an exhaustive catalog for $n = 5$, many entries of which would be straightforward extensions of earlier cases. Instead, we shall restrict attention to a single especially interesting example.

TABLE I

Singularities in the rigid disk and sphere pair distribution functions. The listed r_{12}/a values are arranged in ascending order for each n

n	disks and spheres	spheres only
1	2	
2	$3^{1/2}$	
	2	
	3	
3		$2^{3/2}/3^{1/2}$
	$3^{1/2}$	
	2	
	$3^{1/2} + 1$	
	3	
	4	
4		$2^{1/2}$
		$2^{3/2}/3^{1/2}$
		5/3
	$3^{1/2}$	
	2	
		$3^{1/2} + 2^{-1/2}$
		$(2^{3/2}/3^{1/2}) + 1$
	$7^{1/2}$	
	$3^{1/2} + 1$	
	3	
	$3^{1/2} + 2$	
	4	
	5	

For the first time, with five movable particles, it is possible completely to encircle one of the fixed particles. This situation is shown in Fig. 7, and occurs when $r_{12} = a$. For both rigid disks and spheres, the quantity shown in Eq. (2.8),

$$y^{-2} \exp[\beta\varphi(r_{12})]\, \rho^{(2)}(\mathbf{r}_1, \mathbf{r}_2), \tag{4.10}$$

is well-defined for all $0 \leqslant r_{12} \leqslant a$, but the existence of the configuration of Fig. 7 raises the possibility that $r_{12} = a$ is a singular point of this function. This is clearly the case for rigid disks, since region $\mathbf{R}_5$ has boundary points corresponding to the six simultaneous contacts shown as solid lines in Fig. 7 if and only if $r_{12} \leqslant a$.

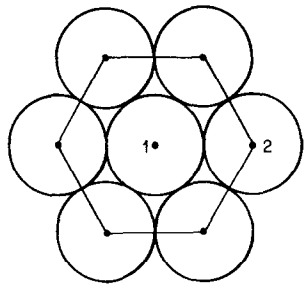

FIG. 7. Particle-encircling contact set for $n = 5$.

In the rigid sphere case, the reason for singular behavior at $r_{12} = a$ is slightly different, but no less compelling. The relevant distinction now is whether or not the contact chain can move without collision over the fixed pair (1, 2) in a "skiprope" mode. Indeed one easily sees that this mode is possible only when $r_{12} \leqslant a$. When r_{12} exceeds a, the set of boundary points for simultaneous contact along the chain (for fixed order of movable particles) is singly connected; however, when r_{12} decreases below a, this set becomes doubly connected. The resulting change in boundary set topology at $r_{12} = a$ surely heralds singular behavior there.

The existence of a singularity in the function (4.10) at $r_{12} = a$ is highly significant. When viewed from the standpoint of functional Taylor series expansions [14], one sees that the Percus–Yevick integral equation for rigid disk and sphere $\rho^{(2)}$'s attempts to extrapolate these functions for $r_{12} \geqslant a$ into the region $0 \leqslant r_{12} < a$. The result of this extrapolation, which predicts function (4.10) over this inner region, allows construction of the "direct correlation function". The singularity at $r_{12} = a$ alone dooms this attempt to somewhat limited accuracy. It seems very noteworthy that on the one hand the Percus–Yevick theory fails to describe solid

phases for disks or spheres [15], while on the other hand the hexagonal grouping shown in Fig. 7 for deduction of the $r_{12} = a$ singularity occurs ubiquitously in close-packed crystals both of spheres and disks.

We now can supplement the set (4.6) of neighbor distances with the first-neighbor distance itself. These disk crystal distances of course also occur in the several close-packed sphere crystals, for which Fig. 3(c) actually exhibits particles 1 and 2 at a characteristic neighbor separation. In a fuller analysis than we can present here, one would expect therefore to find all sphere neighbor distances in all close-packed structures to be singular points of $\rho^{(2)}$.

5. Random Packings

From information thus far adduced, it is clear that $\rho^{(2)}$ singularities must occur more and more closely spaced as r_{12} increases. The neighbor distance distributions for the close-packed lattices alone have this property. However, the same behavior can also be argued to obtain from fully extended chains of movable particles consisting of arbitrary sequences of single contacts [as in Fig. 2(a)] and parallel path pairs [Fig. 2(b)]. These extended contact chains all have lengths of the form

$$r_{12} = (A + 3^{1/2}B)a, \tag{5.1}$$

where A and B are nonnegative integers, and each will provide a singular point. Since $3^{1/2}$ is irrational, the nonintegral (or "fractional") parts of $A + 3^{1/2}B$ must take on an infinite number of distinct values which are distributed uniformly between 0 and 1 [16]. This implies the increasing density claimed as $r_{12} \to \infty$.

The knowledge that singularities in $\rho^{(2)}$ become densely distributed as $r_{12} \to \infty$ still leaves uncertain the possibility that enough singularities at finite r_{12} will tend to arise $n \to \infty$ so that the complete set of singular points is everywhere dense for $0 \leqslant r_{12} < \infty$. We wish now to argue that this possibility in fact is realized.

The key feature in our argument is the existence of a multiplicity of random disk and sphere packings for large n. These packings generally fail to show any long-range regularity. Random packings have been studied for insight into the nature of liquids [17, 18], and in the course of such investigations their average densities have been determined both for disks [19] and spheres [20].

Figure 8 presents a representative random disk packing for $n = 56$. For that packing a set of contact constraints has been chosen, and has been indicated as before by solid lines connecting disk centers. As a bit of experimentation readily shows (with pencil and paper, or coins on a flat surface), there are many ways of surrounding particles 1 and 2 at arbitrary separation r_{12} with a random packing. Subsequently, of course, there are again many choices possible for contact sets with each packing.

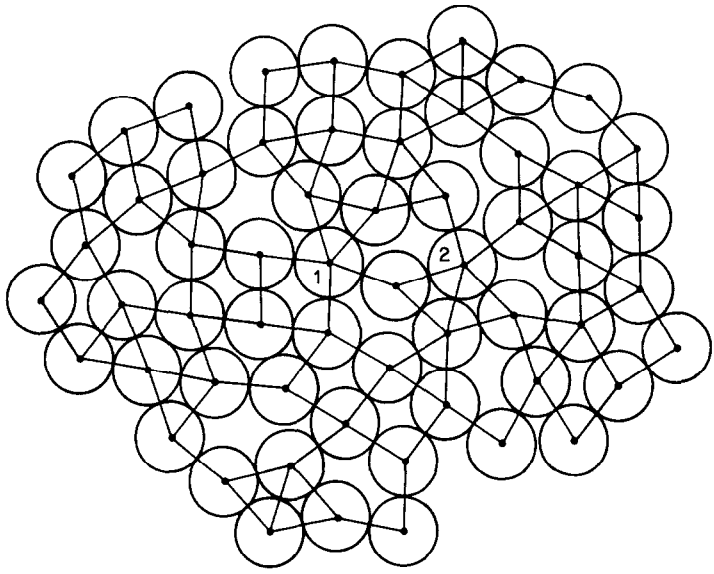

FIG. 8. Random disk packing for $n = 56$. The solid lines represent contacts which are to be maintained as r_{12} varies.

The packing, plus contact constraint set, constitutes generally a very complicated mechanical linkage. Except in very unusual cases [21] this linkage will permit r_{12} to vary somewhat without breaking contacts or forcing overlaps between particle pairs. But if n is large (it has no upper limit so far as our argument is concerned) and if particles 1 and 2 are buried within the center of the random aggregate as in Fig. 8, the expected range of r_{12} variation will be very small. This r_{12} variation will either bring a close pair into contact, or will stretch a chain of contacts to maximum extension. In a very large aggregate it is virtually certain that a very close pair exist not quite in initial contact, or that a nearly completely extended chain present itself.

The endpoints of r_{12} variation for each random packing must be $\rho^{(2)}$ singularities, since they are singularities of the associated X_n. This latter fact is true due to occurrence of $\mathbf{R}_n$ boundary points for the chosen simultaneous contact set only over the small accessible r_{12} range. It therefore seems that for any r_{12} in $0 \leqslant r_{12} < \infty$ (we permit here only the particles 1 and 2 to interpenetrate) there will be $\rho^{(2)}$ singularities that are arbitrarily close to that r_{12} value. In other words, the full set of $\rho^{(2)}$ singularities is dense throughout the entire range $0 \leqslant r_{12} < \infty$.

For the most part, the singularities that are manifest in $\rho^{(2)}$ are very weak, and imply discontinuities only in very high-order derivatives of this function with respect to r_{12}. Indeed it has been empirically known for some time that disk and

sphere distribution functions were quite "smooth". The dense distribution of singularities, regardless of how weak, nevertheless implies that the disk and sphere $\rho^{(2)}$'s are nowhere analytic in the variable r_{12}.

6. Discussion

Although it has been the properties of the pair distribution functions $\rho^{(2)}$ which have formed the subject of this paper so far, the analysis can be readily adapted to higher order distribution functions $\rho^{(3)}$, $\rho^{(4)}$, $\rho^{(5)}$, $\cdots$. One would ultimately conclude that each of these functions was nowhere analytic in their spatial variables r_{ij}, at least for densities that have a convergent virial expansion.

We have already noted the difficulty posed by $\rho^{(2)}$ singularities for the Percus–Yevick integral equation. The closely related "scaled particle theory" [8, 9] is is also affected by our results, since it uses each of $\rho^{(2)}$, $\rho^{(3)}$, $\rho^{(4)}$,... to construct its central quantity, the contact correlation function $G(\lambda)$ for a variably-sized sphere [radius $(\lambda - \frac{1}{2})a$]. Evidently the connection established by the scaled particle theory will not permit $G(\lambda)$ to be analytic in λ for any $\frac{1}{2} \leqslant \lambda < \infty$. The Laurent series that have been used to represent $G(\lambda)$ in this range therefore have a fundamental limitation. In order to improve significantly upon the scaled particle theory, explicit consideration will have to be given the more important singularities in the range $\frac{1}{2} \leqslant \lambda < \infty$, perhaps by splicing together several suitable analytic functions of λ to represent $G(\lambda)$.

Since it has been based on the y power series (2.8), our argument thus far has strictly speaking been relevant only to the disk and sphere fluid phases [22]. Nevertheless, analogous results should apply to the pair distribution function in the solid phase, $\rho^{(2)}(\mathbf{r}_1, \mathbf{r}_2)$, which will now generally depend on more than just the scalar spatial variable r_{12}. One first recognizes that the important terms in definition (2.1) for the solid's $\rho^{(2)}$ will cluster sharply around $N = \bar{N}$, where $\bar{N}$ is the average number of particles in V at the given solid-phase absolute activity y. Now in the $V \to \infty$ limit (constant y), it will always be possible to find configurations of movable particles with some finite number n in a randomly packed aggregate around 1 and 2, and the others moved cooperatively outward from the aggregate's vicinity. However, it is precisely these randomly packed configurations for each finite n which produce $\rho^{(2)}$ singularities. Therefore, we are forced to conclude that the solid-phase $\rho^{(2)}(\mathbf{r}_1, \mathbf{r}_2)$ has a dense set of singularities in at least its scalar radial variable r_{12}. At present we can say nothing about singularities in other configurational variables for fixed r_{12}.

It is worth appending here the observation that the strength of the individual singularities for the most part goes to zero as $y \to \infty$. In this high-compression limit it becomes very costly on a free energy basis to effect the necessary cooperative

motion around fixed particles 1 and 2 which results in a very unnatural (for the crystal) random packing. Therefore, the limiting high-compression pair distribution functions (for which y tends to infinity *before* V tends to infinity) that may be studied through the convex geometry of limiting polytopes [23] need not be everywhere nonanalytic.

The dense singularities which apply to rigid disk and sphere $\rho^{(2)}$'s have no analog for one-dimensional rigid rods. It is obvious that no one-dimensional version exists for the diverse and numerous random packings that are possible in two and three dimensions. The known rigid rod $\rho^{(2)}$ in fact is piecewise analytic, with singularities corresponding to chains of contacting rods, the only possibility [24].

It is worthwile remarking finally on the implication of our results for computational statistical mechanics. Often, of course, the numerical distinction between analytic functions, and smooth but nowhere analytic functions, would be barely perceptible. This situation may largely be the case for disk and sphere pair distribution functions determined by Monte Carlo or molecular dynamics computations. Nevertheless it seems likely that a few of the singularities which we uncovered in Section 4 for small n (and which recur in each succeeding order) will have significant effects. If the singular values of r_{12} which have greatest importance are a, $3^{1/2}a$, and $2a$, for instance, it would be valuable to make separate polynomial fits to $\rho^{(2)}$ over the intervals $a \leqslant r_{12} \leqslant 3^{1/2}a$ and $3^{1/2}a \leqslant r_{12} \leqslant 2a$ (while enforcing continuity) for the purposes of accurate data representation. By a suitable extension of our arguments, it should be possible to identify the derivative order which first becomes discontinuous at each singularity, so that adroit interval fits could predict the numerical magnitude of those discontinuities as a function of density.

In spite of clever experimentation [20], not too much is yet known about random disk or sphere packings. Since these random packings play such a central role, this ignorance of their rigorous mathematical properties is one reason the present heuristic argument cannot be elevated to the status of impeccable proof. Computer construction of random packing ensembles would be a valuable adjunct to the present work, employing either a variational technique [19] or some suitable alternative. Among other properties, one should seek to determine the average density of these jammed random packings, their average contact number and radial pair distribution, and their movement freedom (as in Section 5) when a free surface is present and various contact constraints maintained.

ACKNOWLEDGMENT

The author is deeply grateful to the late Professor Zevi W. Salsburg for the pleasure of extended collaboration on the statistical mechanics of rigid-particle models. The central concepts in the present paper grew largely from that collaboration.

REFERENCES

1. B. J. ALDER AND T. E. WAINWRIGHT, *Phys. Rev.* **127** (1962), 359.
2. W. G. HOOVER AND F. H. REE, *J. Chem. Phys.* **49** (1968), 3609.
3. F. H. REE AND W. G. HOOVER, *J. Chem. Phys.* **46** (1967), 4181.
4. F. H. STILLINGER, Z. W. SALSBURG, AND R. L. KORNEGAY, *J. Chem. Phys.* **43** (1965), 932.
5. W. G. RUDD, Z. W. SALSBURG, A. P. YU, AND F. H. STILLINGER, *J. Chem. Phys.* **49** (1968), 4857.
6. B. J. ALDER, W. G. HOOVER, AND T. E. WAINWRIGHT, *Phys. Rev. Letters* **11** (1963), 241.
7. B. J. ALDER, W. G. HOOVER, AND D. A. YOUNG, *J. Chem. Phys.* **49** (1968), 3688.
8. H. REISS, H. L. FRISCH, AND J. L. LEBOWITZ, *J. Chem. Phys.* **31** (1959), 369.
9. E. HELFAND, H. L. FRISCH, AND J. L. LEBOWITZ, *J. Chem. Phys.* **34** (1961), 1037.
10. M. S. WERTHEIM, *J. Math. Phys.* **5** (1964), 643.
11. D. RUELLE, "Statistical Mechanics," pp. 85, 90, W. A. Benjamin, New York, 1969.
12. T. L. HILL, "Statistical Mechanics," p. 211, McGraw-Hill, New York, 1956.
13. B. R. A. NIJBOER AND L. VAN HOVE, *Phys. Rev.* **85** (1952), 777.
14. J. K. PERCUS, *Phys. Rev. Letters* **8** (1962), 462.
15. P. HUTCHINSON, *Mol. Phys.* **13** (1967), 495.
16. I. NIVEN, "Diophantine Approximations," p. 24, Interscience, New York, 1963.
17. J. D. BERNAL, *Proc. Roy. Soc.* **A280** (1964), 299.
18. J. D. BERNAL AND J. L. FINNEY, *Discussion Faraday Soc.* **43** (1967), 62.
19. F. H. STILLINGER, E. A. DIMARZIO, AND R. L. KORNEGAY, *J. Chem. Phys.* **40** (1964), 1564.
20. G. D. SCOTT AND D. M. KILGOUR, *J. Phys. D* **2** (1969), 863.
21. One might have accidentally chosen r_{12} to be precisely a close-packed neighbor distance, and then proceeded to complete a close-packed structure with all nearest neigbors required to remain in contact. The existence of such exceptions does not affect the outcome of our argument.
22. Although the virial series may fail to converge all the way up to the transition density, it would be very odd indeed for $\rho^{(2)}$ nonanalyticity within the convergence radius suddenly to switch to piecewise analyticity, still in the fluid phase. After all, the thermodynamic functions manifest no corresponding symptom. We must therefore suppose that $\rho^{(2)}$ nonanalyticity applies throughout the entire fluid range of densities, regardless of the precise virial series convergence radius.
23. F. H. STILLINGER AND Z. W. SALSBURG, *J. Stat. Phys.* **1** (1969), 179.
24. Z. W. SALSBURG R. W. ZWANZIG AND J. G. KIRKWOOD *J. Chem. Phys.* **21** (1953), 1098.